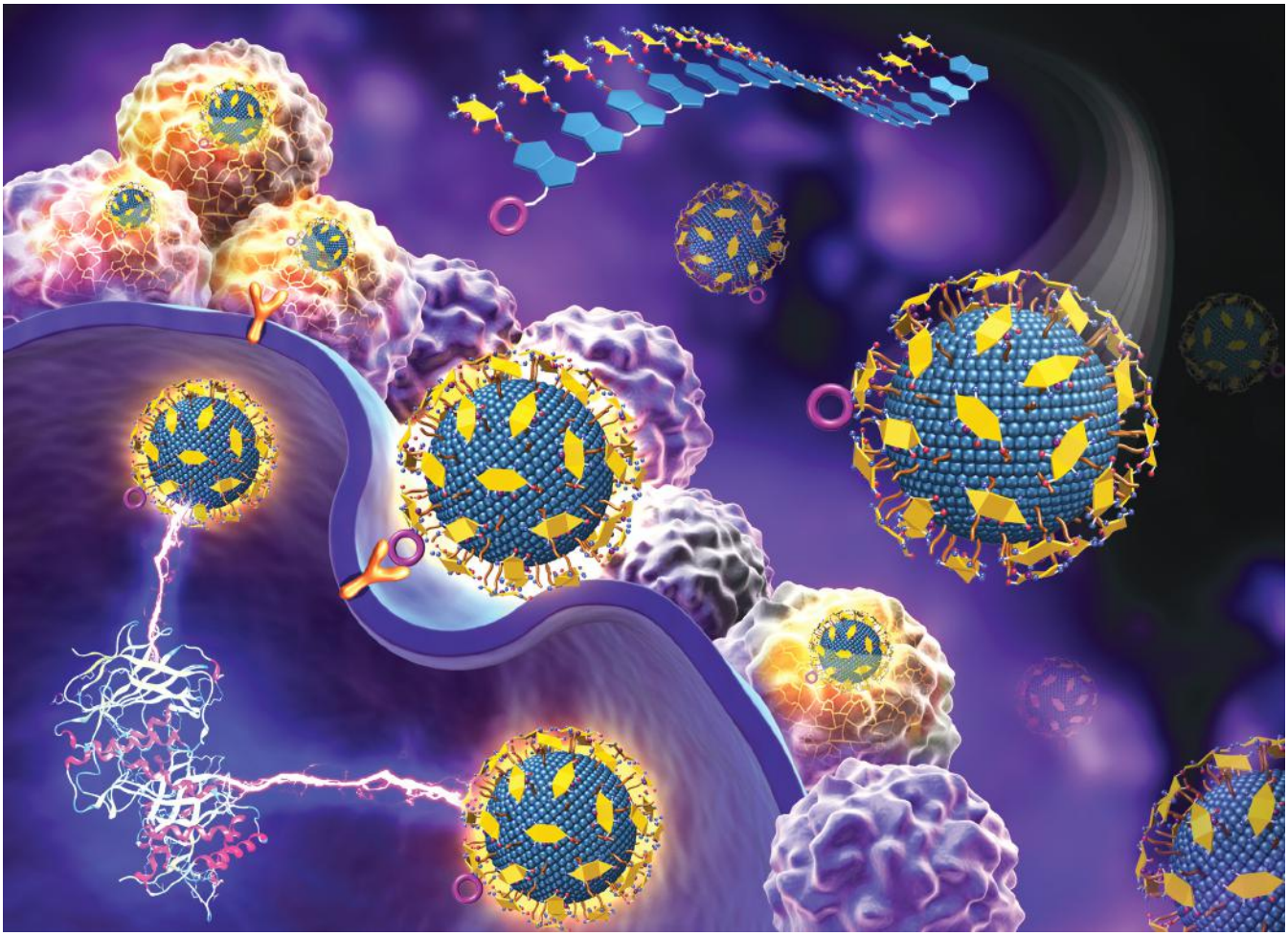

Highlighting a research article from the Carbohydrate Research group at Ocean University of China.

End-functionalised glycopolymers as glycosaminoglycan mimetics inhibit HeLa cell proliferation

This article introduces the polymer–peptide conjugates prepared by post-modification and end-functionalisation with distinct sulphation patterns, and these glycoconjugates could self-assemble to form nanoparticles with inhibition of heparanase as well as tumour cell proliferation.

As featured in:

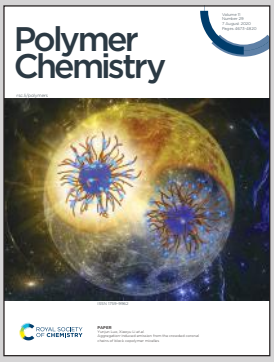

See Chao Cai, Ming Liu, Guangli Yu *et al.*, *Polym. Chem.*, 2020, **11**, 4714.

ROYAL SOCIETY OF CHEMISTRY

rsc.li/polymers

Registered charity number: 207890

Polymer Chemistry

ROYAL SOCIETY OF CHEMISTRY

PAPER

View Article Online
View Journal | View Issue

Cite this: *Polym. Chem.*, 2020, **11**, 4714

End-functionalised glycopolymers as glycosaminoglycan mimetics inhibit HeLa cell proliferation†

Chendong Yang,‡[a] Lei Gao,‡[a] Meng Shao,[a] Chao Cai, *[a,b] Lihao Wang,[a,b] Yifan Chen,[a] Jianghua Li,[a] Fei Fan,[a] Yubing Han,[a] Ming Liu,*[a,b] Robert J. Linhardt [c,d] and Guangli Yu*[a,b]

The glycosaminoglycans (GAGs) on cell surfaces play significant roles during cancer development, and the heparanase activity is strongly implicated in the structural remodeling of the extracellular GAG matrix, potentially leading to tumour cell invasion. Polymer–protein/peptide conjugates are one of the most promising approaches for anticancer therapy due to their controllability, biocompatibility, and targeting properties. In this study, distinct and well-defined glycopolymer–peptide conjugates, mimicking the multivalent architecture found in GAGs, were synthesised for targeting and killing tumour cells. Regioselectively sulphated galactosamine derivatives were chemically synthesised, and six GAGs-mimetic glycopolymers were generated by post-modification based on the ring-opening metathesis polymerization (ROMP). The glycopolymers with diverse galactosamine sulphation patterns showed significant inhibitory effects on heparanase. Glycopolymers decorated with 3,4,6-*O*-sulphated GalNAc exhibited the highest activities, inhibiting heparanase as well as tumour cell proliferation. We demonstrated that a novel glycopeptide mimetic, derived from end-functionalised conjugation of the iRGD peptide on the glycopolymer, could effectively enter HeLa cells and inhibit signalling pathways involved in tumour cell proliferation. These findings should promote the development of novel glycomimetics for specific tumour-targeted therapies.

Received 14th March 2020,
Accepted 25th June 2020

DOI: 10.1039/d0py00384k

rsc.li/polymers

Introduction

Glycosaminoglycans (GAGs) are a class of linear polysaccharides composed of variably sulphated, disaccharide repeating motifs, including amino and acidic saccharides.[1] GAGs participate in diverse biological processes, such as cell–cell interactions, signal transduction, cancer metastasis, angiogenesis, and central nervous system (CNS) development.[2] Many studies suggest that the structural diversity of GAGs, including chain length, stereochemistry, disaccharide composition, and sulphation patterns, are the basis for the interaction between GAGs and multiple protein ligands.[3]

Cancer is a major threat to human health according to worldwide cancer statistics[4] and there is an urgent need for new anti-tumour drugs. Previous studies have shown that the sulphation pattern of GAGs on the surface of cancer cells are dramatically different from those of healthy cells and that there is a clear correlation between the expression of heterogeneous GAGs and cancer progression.[5] A higher expression of the GAG, chondroitin sulphate E, has been observed on the surface of ovarian and pancreatic cancer cells, which influences the metastatic potential of neoplastic cells.[6] These GAGs interact with various protein factors, including basic fibroblast growth factor (BFGF), vascular endothelial growth factor (VEGF), heparin-binding epidermal growth factor-like growth factor (HB-EGF), and the receptor for advanced glycation end-products (RAGE), participating in tumour growth and metastasis.[7] Sulphated GAGs, isolated from marine sources, have anticancer activity against HeLa cells resulting in 18.65%–66.13% inhibition at 50–250 μg mL^{-1}.[8] Moreover, the Borsig group found that fucosylated chondroitin sulphate (FucCS) iso-

[a]*Key Laboratory of Marine Drugs, Ministry of Education & Shandong Provincial Key Laboratory of Glycoscience and Glycotechnology, School of Medicine and Pharmacy, Ocean University of China, Qingdao 266003, China. E-mail: caic@ouc.edu.cn, lmouc@ouc.edu.cn, glyu@ouc.edu.cn*
[b]*Laboratory for Marine Drugs and Bioproducts, Pilot National Laboratory for Marine Science and Technology (Qingdao), Qingdao 266237, China*
[c]*Department of Chemistry and Chemical Biology, Center for Biotechnology and Interdisciplinary Studies, Rensselaer Polytechnic Institute, Troy, NY, 12180, USA*
[d]*Department of Chemical and Biological Engineering, Center for Biotechnology and Interdisciplinary Studies, Rensselaer Polytechnic Institute, Troy, NY, 12180, USA*
†Electronic supplementary information (ESI) available: Materials, preparation and characterization. See DOI: 10.1039/d0py00384k
‡These authors contributed equally.

lated from sea cucumber inhibits lung colonization by adenocarcinoma MC-38 cells in an experimental metastasis model in mice.[9] Multiple studies have demonstrated the antitumour activity of natural GAGs, but their structure–activity relationship is still unclear due to the challenges in structurally characterizing GAG polysaccharides. Thus, mechanistic studies on their antitumour activities remain quite limited.

Heparanase, an *endo*-β-D-glucuronidase,[10] is expressed at high levels in various human tumour cells and specific tissues, such as mammalian placenta. This expression is related to the activation of multiple growth factors, which play an important role in leading tissue repair, cell adhesion, growth, proliferation and differentiation, cancer, angiogenesis, neurite outgrowth, and inflammatory-related diseases.[11] Studies clearly demonstrate that heparanase can induce the release of heparan sulphate (HS)-bound growth factors bFGF and VEGF, thereby promoting the formation of a HS-FGF-FGFR complex, which then activates FGF receptor dimerization and related signalling pathways leading to uncontrolled proliferation and dissemination of tumour cells.[12] Thus, targeting heparanase interactions with potent antagonists, such as GAG (especially HS) mimics, can inhibit growth/dissemination of cancer cells by reducing heparanase-related signalling pathways.[13]

Multivalent mutual recognition of saccharides in biological targets can modulate multiple important cell functions.[14] Therefore, GAG-mimicking glycopolymers show great promise as heparanase antagonists. Recently, glycopolymers based on natural GAG structures have demonstrated the critical biological activities of GAGs. Chaikof developed a cyanoxyl-mediated free-radical polymerization for the assembly of glycopolymers with fully sulphated GlcNAc/lactose (Lac), and this sulphated Lac-polymer effectively promoted the combined activities of FGF-1 and FGF-2.[15] Moreover, well-defined pendant saccharides provide an excellent strategy for exploring the relationship between sulphation patterns and the diverse biological activities of GAGs. The Miura group reported that the 3,4,6-*O*-sulphation pattern of GlcNAc-glycopolymer was significant to BACE-1 inhibition and VEGF binding affinity.[16] Our group recently also found that HS glycopolymers, with overall *O*-sulphated trisaccharide motifs, showed a potent affinity to RAGE.[17] Meanwhile, a range of glycopolymer inhibitors of heparanase with different pendant HS disaccharides have been well assembled by Nguyen.[18] In addition, protein/peptide–polymer conjugates[19] have been extensively developed for the desired applications in reducing immunogenicity, and improving bioactivity as well as targeting specific sites, *etc*. This inspired us to design and synthesise novel and specific glycopeptide conjugate for inhibiting heparanase and tumour cell proliferation.

Here, we report a systematic study on the inhibition of tumour cells by glycopolymers with galactosamine derivatives having specific sulphation patterns. Six novel glycopolymers were synthesised and evaluated for their inhibitory effects against tumour cells *in vitro*. Our results showed that the glycopolymer with 3,4,6-*O*-sulphated groups showed the highest inhibitory activity against heparanase and tumour proliferation. In addition, a functionalised terminating agent was designed to provide a concise approach to obtain end-functionalised glycopeptide mimetics with the iRGD peptide. End-functionalised glycopeptide mimetics could efficiently enter HeLa cells in a time-dependent manner, inhibiting the proliferation of HeLa cells through blocking the heparanase-related signalling pathways. The results show that the end-functionalised glycopeptide mimetics are potent modulators of tumour cells by inhibiting heparanase activity.

Results and discussion

Synthesis of diverse glycopolymers with specific sulphation patterns

A fully protected aminogalactose **7**, prepared from D-galactosamine hydrochloride as a starting material, was used to synthesise six *N*-acetyl and *N*-sulpho-galactosamine derivatives by protecting group manipulation and regioselective sulphation (Scheme 1). The ester-protecting groups on monosaccharide **7** were removed with sodium hydroxide in 1,4-dioxane to obtain unprotected galactosamine **19** (Scheme S1, ESI†). Taking advantage of the different reactivity between amino and hydroxyl groups, regioselective acetylation and sulphation were employed to provide the non-sulphated **20**, *O*-sulphated **21**, *N*-sulphated **22**, and persulphated **23** (Scheme S1, ESI†), respectively, which was also confirmed by NMR spectra. Four monosaccharide substrates with specific sulphation patterns

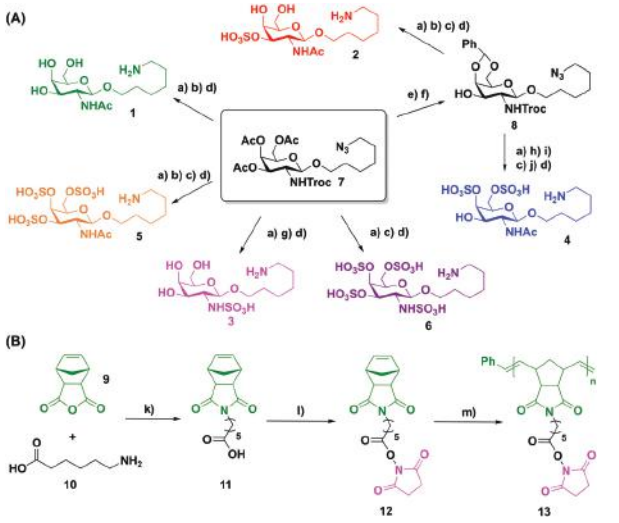

Scheme 1 Synthesis of diverse substrates with specific sulphation patterns (A) and polymer backbone (B). Reagents and conditions: (a) 0.6 M NaOH in water/1,4-dioxane (1 : 1), 80 °C, 1 h. (b) Et_3N, Ac_2O, CH_3OH, rt, 1 h. (c) SO_3·Et_3N, DMF, 50 °C, 10 h. (d) $Pd(OH)_2/C$, H_2, CH_3OH/H_2O (1 : 1), rt, 2 h. (e) CH_3ONa, CH_3OH, rt, 1 h. (f) α,α-Dimethoxytoluene, CSA, CH_3CN, rt, 3 h. (g) SO_3·Et_3N, Et_3N, Py, rt, 6 h. (h) Ac_2O, Py, rt, 12 h. (i) 70% CH_3COOH in H_2O, 60 °C, 2 h. (j) CH_3ONa, CH_3OH, −5 °C, 6 h. (k) Et_3N, toluene, 120 °C, 5 h. (l) EDC, *N*-hydroxysuccinimide, DCM, rt, 5 h. (m) Grubbs 3rd, DCM, −78 °C–rt, 1 h.

were obtained as **1**, **3**, **5**, and **6** (Scheme 1 and S1, ESI†) after the reduction of azido to amine group.

For the preparation of 3-*O*-sulphated **2** and 4,6-*O*-sulphated **4**, intermediate **8** (Scheme S1, ESI†) was obtained by following the removal of esters, benzylidene protection on aminogalactose **7**. The troc group on intermediate **8** was removed and regioselective acetylation to provide **24** and **26**. After removal of benzylidene on **24** using 70% CH_3COOH, 4,6-*O*-sulphation was later achieved with $SO_3{\cdot}Et_3N$ in DMF, but we also found that the presence of sulphate groups made it difficult to fully cleave 3-*O*-acetyl groups. Unfortunately, increasing amounts of the sodium methoxide led to the removal of sulphate groups. We then used a low-temperature reaction apparatus, and 3-*O*-acetyl groups group is smoothly removed without any unexpected cleavage at −5 °C (Scheme S1, ESI†). Meanwhile, the selective sulphation at C3 position on **26** was acquired by the same approach as above-mentioned. Global hydrogenation was subsequently performed to afford the key building blocks 3-*O*-sulphated **2** and 4,6-*O*-sulphated **4**.

Glycopolymers have been developed as potential high potency inhibitors of glycosidases and their side-chain moieties play important roles in their activities. NHS ester-substituted polymers were generated by ROMP and glycopolymers were synthesised through a post-polymerization strategy to achieve concise assembly of glycopolymer *in situ*.[20] Norbornene anhydride **9** was coupled with 6-aminocaproic acid to give **11** in a 95% yield and the NHS ester **12** was generated by EDC and *N*-hydroxysuccinimide. The polymer backbone **13** was assembled by the NHS ester **12**, using ruthenium initiator (Grubbs 3rd) in dichloromethane (Scheme 1B). The successful synthesis of **13** was then determined by ^{1}H NMR with alkene signals shifting from 6.44 ppm to 5.57–5.94 ppm (Fig. 2). The degree of polymerization was well controlled by the ratio between the monomer and catalyst, exactly determined by NMR analysis to be 50 DP (Tables 1 and S23, and Fig. S31, ESI†). The molecular weight of the polymer was also confirmed by NMR spectra.

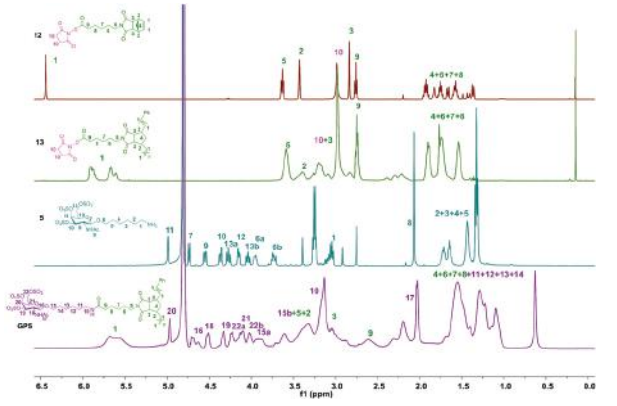

Fig. 2 ^{1}H NMR spectra comparison of the NHS ester (**12**), polymer backbone (**13**) in $CDCl_3$, 3,4,6-*O*-sulphated monosaccharide (**5**), and the relative glycopolymer (**GP5**) in D_2O.

Table 1 Properties of the synthesised glycopolymers

No.	Sugar type	M_n (NMR)[a]	Rh[b] (nm)	Zeta-potential[b] (mV)	Yield[c]
GP1	1	38 kDa	323	−9.21	92%
GP2	2	36.7 kDa	363	−13.5	88%
GP3	3	28.7 kDa	531	−5.82	76%
GP4	4	32 kDa	285	−26.6	80%
GP5	5	32 kDa	266	−19.8	90%
GP6	6	32 kDa	182.5	−23.5	87%

[a] Molecular weight (M_n) were determined by ^{1}H NMR integration. [b] Rh and zeta potential were measured with a Zetasizer Nano ZS90 instrument. [c] Yield% = [(actual weight of glycopolymer)/(weight of fully substituted glycopolymer)] × 100%.

Diverse glycopolymers were prepared by post-modification of the polymer backbone with amidation on different galactosamine building blocks. Prior reports had suggested amidation could be handled in a PBS buffer/DMF solvent, but we found that the hydrophobic polymer backbone and hydrophilic galactosamine derivatives could not dissolve simultaneously. Therefore, we developed a DMF/H_2O (7 : 1) co-solvent mixture for the coupling reaction. All of the components were fully dissolved in this homogeneous system, and the reaction was successfully promoted by triethylamine (Et_3N) as a proton scavenger. Accordingly, the ^{1}H NMR spectra indicated successful construction of glycopolymers after the coupling and purification steps. The mole fraction of sulphated monosaccharide was determined through the comparison of the protons at the anomeric position and the alkene groups (Fig. 2 and S27–S32, ESI†). With the six sulphated galactosamine building blocks (**1–6**) in hand, we next designed and synthesised the glycopolymers (**GP1–GP6**) with distinct sulphation patterns (Table 1). The molecular weights were determined by the integration analysis of ^{1}H NMR spectra for all glycopolymers (Table 1 and Fig. S25–S30, ESI†). All of the glycopolymers were found to be self-assembled into nanoparticles that could be potentially attributed to the diblock amphiphilic copolymers composed of the hydrophobic backbone and hydrophilic sugar moieties. The size and morphology of the resulting glycopolymers were characterised by dynamic light scattering (DLS) and transmission electron microscopy (TEM). As shown in Fig. 1 and Table 1, glycopolymers evolved to form spherical nanomicelles with diameters of 182.5–531 nm at pH 7.2. In addition, the stability of nanomicelles was evaluated by zeta potential at pH 7.2, and their values were measured to be −5.82 to −26.6 mV (Table 1), guaranteeing the stability of the nanomicelles. Interestingly, **GP5** with moderate zeta potential value showed the highest bioactivity, which is consistent with the reference results[16a] possibly due to the charge repulsion at higher sulphate content.

Screening for heparanase inhibitory activity and cytotoxic activity *in vitro*

Heparanase, through the cleavage of heparan sulphate proteoglycans (HSPGs) releases HS, which plays an important role in

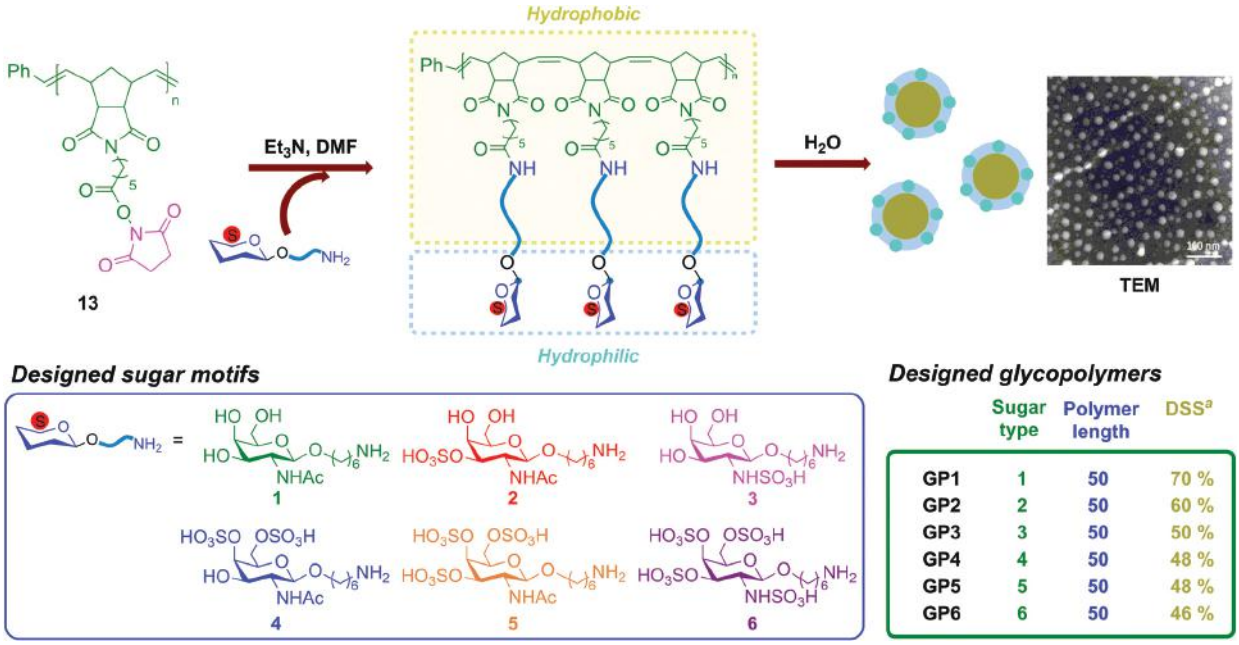

Fig. 1 Schematic illustration of the preparation of various glycopolymers by "post-modification" strategy. [a] DSS = degree of sugar substitution.

Table 2 Inhibition of heparanase by sulphated glycopolymers using a TR-FRET Assay

Entry	Compounds	IC_{50} [a]
1	**GP-1**	2.13 μM
2	**GP-2**	456 nM
3	**GP-3**	289 nM
4	**GP-4**	387 nM
5	**GP-5**	5.39 nM
6	**GP-6**	263 nM
7	DS	1.15 μM
8	LMWH[b]	18.1 nM
9	Heparin	3.74 nM

[a] Inhibition of heparanase was assessed by *in vitro* TR-FRET assay against fluorescently-tagged HS. [b] LMWH = low molecular weight heparin.

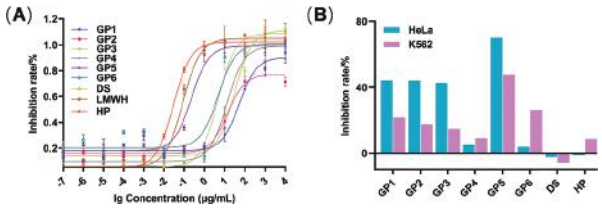

Fig. 3 (A) Inhibition of heparanase by diverse sulphated glycopolymers using a TR-FRET assay (n = 3). (B) Screening for cytotoxic activity of HeLa and K562 cells with **GP1–GP6**, DS, and HP (n = 3).

tumour growth and metastasis. We focused on the inhibition of heparanase activity by glycopolymers with different sulphation patterns,[8–10] which could be highly correlated to the tumour inhibitory activity. The inhibitory effect was assessed using a Time-Resolved Fluorescence Resonance Energy Transfer (TR-FRET) assay. The results showed that heparanase inhibitory activity is closely related to the pattern and degree of sulphation (Table 2 and Fig. 3A). Non-sulphated glycopolymer **GP1** were devoid of any significant heparanase inhibitory capacity (IC_{50} = 2.13 μM for **GP1**, Table 1, entry 1 and Fig. 3A), while the sulphated glycopolymers exhibited higher affinity with heparanase. Notably, glycopolymer **GP5** with 3,4,6-*O*-sulphation had the highest heparanase inhibitory effect with IC_{50} value at 5.39 nM (Table 2, entry 5), which is comparable to heparin at 3.74 nM (Table 2, entry 9). The glycopolymer with *N*-sulphation showed relatively lower heparanase inhibition than *N*-acetylated glycopolymer, but it also showed higher inhibitory effect than other glycopolymers. The results obtained in this study is comparable with the report from Miura's group[16c] as well. 3,4,6-*O*-Sulfated and *N*-acetylated glycopolymers possess the highest inhibitory effects.

We screened glycopolymers by measuring their proliferation inhibitory activities against HeLa cell and K562 cell to demonstrate the potential antitumour activity of glycopolymers. The influence of the sulphation mode on the cytotoxic activity was evaluated along with synthetic glycopolymers, natural dermatan sulphate (DS), and heparin. **GP2** and **GP3** with monosulphated groups only showed moderate inhibition similar to non-sulphated glycopolymer **GP1**. In contrast, **GP5** with 3,4,6-*O*-sulphated groups showed significant cytotoxicity compared to other glycopolymers (Fig. 3B), which is consistent with the results of heparanase inhibitory activities suggesting that the inhibition of HeLa and K562 cell proliferation could

be potentially induced by heparanase suppression. Interestingly, DS and heparin showed little cytotoxicity towards proliferating tumour cells, possibly due to their dose/concentration dependent effect on cell proliferation *vs.* inhibition. The 3,4,6-*O*-sulphated glycopolymer (**GP5**) exhibits superior ability to kill cancer cells and inhibit heparanase activity. Therefore, the end-functionalised glycopeptide mimetic, 3,4,6-*O*-sulphated GalNAc glycopolymer (**GP5**) was synthesised for subsequent studies.

End-functionalisation of glycopolymer with iRGD peptide

Previous studies indicate that functionalised capping agents containing a symmetric *cis*-olefin could be used for rapid and efficient end-capping of ROMP.[21] This provides an approach for the concise establishment of glycopeptide mimetics with specific properties. Here, we report a terminating agent **16** developed for the capping of a ROMP-derived polymer with maleimide, providing an active site for the coupling with other biological molecules. As depicted in Scheme 2, copper-catalyzed azide–alkyne cycloaddition (CuAAC) of *cis*-butenedioic-bis(6-azidohexyl) ester **15** with 6-(*N*-maleimido)-*N*-(2-propynyl) hexanamide **14** smoothly generated the terminating agent **16**, which was then determined by ^{1}H NMR with the shift from the alkyne signal at 2.22 ppm to the triazoles signals at 7.56 ppm (Fig. S20–S22 and S33, ESI†). Next, the end-functional polymer backbone (50 DP) was formed *via* **16** as a capping agent instead of vinyl ether for terminating the ROMP reaction, and the end-functionalised 3,4,6-*O*-sulphated glycopolymer **GP5-TA** was then synthesised by the abovementioned post-polymerization.

iRGD, a tumour-homing peptide, is mainly composed of arginine, glycine, and aspartic acid that can specifically bind to integrin avβ3 on the tumour endothelium to achieve specific adhesion to tumours. Numerous studies have reported that compounds coupled with iRGD can spread into the tumour parenchyma, thereby increasing its antitumour activity.[22] Therefore, the iRGD peptide was attached to the glycopolymer **GP5-TA** to improve the tumour targeting of the glycopolymers in this study. Finally, the thiol group on the iRGD peptide can effectively react with maleimide to obtain the end-functionalised glycopeptide mimetic **GP5-iRGD** for further evaluation of its antitumour mechanism (Scheme 2).

Anti-tumour mechanism of end-functionalised glycopeptide mimetic

The fluorescent group Cy3 was subsequently introduced into the glycopolymer, and the intracellular fluorescence intensity of **GP5-iRGD** in HeLa cells was detected by flow cytometry to determine whether end-functionalised glycopeptide mimetic **GP5-iRGD** could effectively bind to the tumour cells. Fig. 4A shows that HeLa cells were incubated with **GP5** and **GP5-iRGD** for 4 h, and the significantly stronger fluorescence intensity was detected after incubation with **GP5-iRGD** compared with only **GP5**, suggesting that **GP5-iRGD** have higher cellular uptake efficiency for possessing anti-tumour activity (Fig. 4A). We examined the fluorescence localization of **GP5-iRGD** in cells by confocal microscopy to further determine the cellular distribution of glycopeptide mimetic **GP5-iRGD** in HeLa cells. The results showed that after incubation with **GP5-iRGD** for 4 h, the fluorescence of **GP5-iRGD** clearly appeared in the cytoplasm of HeLa cells; much more fluorescence appeared in the cytoplasm after incubation for 12 h. These results indicated that **GP5-iRGD** was localised to the cytoplasm of HeLa cells with a time-dependent distribution (Fig. 4B and S32, ESI†).

Heparanase can also activate several signalling pathways, including ERK and FGF-FGFR.[23] We evaluated several key signalling molecules by western blot analysis to determine whether **GP5-iRGD** inhibition on heparanase induced the inhibition of its related signalling pathways. Compared with the control group, the phosphorylation levels of ERK were inhibited, suggesting that **GP5-iRGD**-induced heparanase inhibition also inactivated the downstream signalling pathways, while their protein levels were not affected (Fig. 4C and D). We also detected the PI3K/AKT/mTOR signalling pathway, which is an important growth signalling pathway for tumour cells. The activation of AKT, PI3K, and mTOR all decreased after **GP5-iRGD** treatment, while their total protein levels remained the same as before (Fig. 4C and D), suggesting that **GP5-iRGD** also

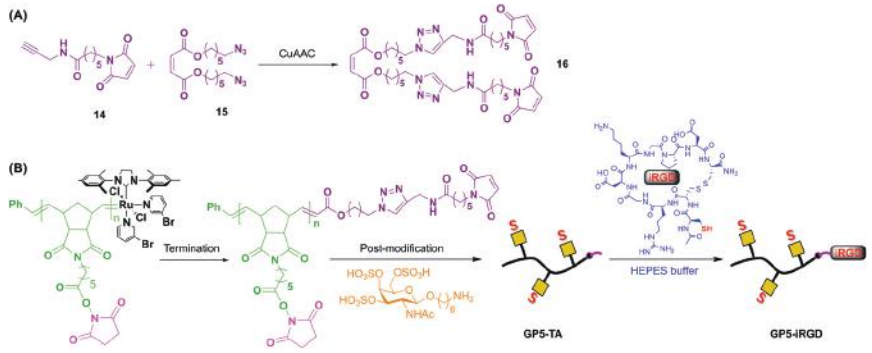

Scheme 2 Synthesis of the terminating agent **16** (A) and end-functionalised glycopeptide mimetic **GP5-iRGD** (B).

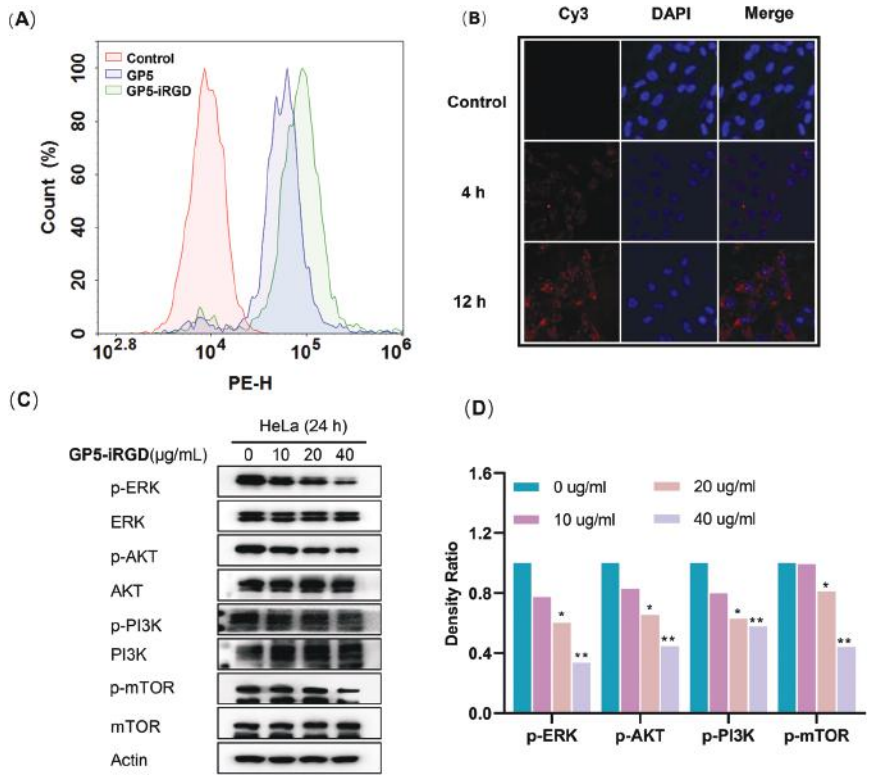

Fig. 4 (A) Flow cytometric analysis of fluorescence intensity in HeLa cells incubated with **GP5** and **GP5-iRGD** (20 μg mL^{-1}) for 4 h. (B) Confocal images of HeLa cells incubated with **GP5-iRGD** (20 μg mL^{-1}) for 4 h and 12 h. (C) **GP5-iRGD** inhibits the activation of HPA downstream and proliferation-related signalling molecules. HeLa cells were treated with different concentrations of **GP5-iRGD**, and western blot was used to detect the signalling molecules. (D) Bar graph shows the decrease in phosphorylation levels of ERK, AKT, PI3K, and mTOR. The values represent the means ± SD. $*P < 0.05$, $**P < 0.01$ *versus* the DMSO vehicle control group. All of the experiments were performed in three replicates ($n = 3$).

inhibited the proliferation and related signalling pathways in HeLa cells.

Conclusion

In this study, we established a rational and concise approach for the development of potential tumour suppressors based on the structure of GAGs. Six glycopolymers decorated with distinct sulphation patterns on galactosamine derivatives were fabricated by post-polymerization strategy. Heparanase and tumour inhibitory activities are closely related to the sulphation patterns and degrees, and the glycopolymer containing 3,4,6-*O*-sulphated GalNAc motifs showed the strongest inhibitory activity on both heparanase and tumour inhibition. We also designed a functionalised terminating agent to obtain the end-functionalised glycopeptide mimetic containing 3,4,6-*O*-sulphated GalNAc, and iRGD as a tumour-targeting peptide. We also demonstrated that the end-functionalised glycopeptide mimetic could successfully enter HeLa cells in a time-dependent manner. The study of the related signalling pathways, including ERK, AKT, PI3K, and mTOR, confirmed the downregulation of their phosphorylation levels during HeLa cell proliferation. We hypothesised that the glycopeptide mimetic could be potentially developed as a novel tumour suppressor through the inhibition of heparanase and related signalling pathways in the future.

Experimental section

General procedure for the preparation of polymer containing NHS ester

A solution of NHS ester **12** in CH_2Cl_2 was stirred at −78 °C for 30 min with argon protection. A stock solution of the Grubbs third catalyst was freshly prepared at 14.2 mg mL^{-1} in dichloromethane. Following the addition of desirable amounts of the catalyst solution, the mixture was stirred vigorously at −78 °C for 20 min, and then stirred at room temperature protected from light. The reaction time for the complete consumption of the monomer was monitored by thin layer chromatography (TLC). At the end of the reaction, excess ethyl vinyl ether was added to quench the reaction, and the mixture was then stirred for 30 min. Following stirring, the excess Et_2O (×5 volume) was added, and a light brown precipitate was formed. The suspension was centrifuged and the ether was then dec-

anted. Repeat the process of centrifuging and decanting to afford the final polynorbornyl NHS ester as a grey solid. The polymer was stored at −20 °C and characterised by ^{1}H-NMR.

General procedure for post-modification of NHS-containing polymer with sugar units

Before the condensation of NHS-containing polymer with sugar units, an NHS-containing polymer (1 eq., based on monomer) was dissolved in 1.4 mL DMF to prepare solution A, and terminal amine functionalised galactosamine (1.2 eq.) was dissolved in 200 μL deionised water to prepare solution B. Afterward, solution A and Et_3N (5 eq.) were added to solution B quickly. The mixture was stirred vigorously under room temperature for 5 h after which TLC indicated full conversion. The mixture was dialyzed against deionised water for 3 days using cellulose membranes with a molecular weight cut-off of 3.5 kDa and lyophilised to obtain the purified glycopolymer as a white powder. The glycopolymers were stored at −20 °C and characterised by ^{1}H-NMR.

TR-FRET heparanase inhibition assay

Heparanase inhibition assays were performed using the heparanase assay toolbox with (human recombinant heparanase 7570-GH). A total of 42 μL of inhibitor solution in Milli-Q water or just Milli-Q water (as a control) and 42 μL of heparanase (5.3 nM, R&D Systems) solution in pH 7.5 tris buffer (consisting of 20 mM Tris-HCl, 0.15 M NaCl, and 0.1% CHAPS) or a buffer blank were added into microtubes and preincubated at 37 °C for 10 min. Next, 84 μL of biotin-heparan sulphate-Eu cryptate (Cisbio, Cat # 61BHSKAA; 0.7 μg mL^{-1} in pH 5.5 0.2 M $NaCH_3CO_2$ buffer) was added to the microtubes, and the resulting mixture was incubated for 60 min at 37 °C. The reaction mixture was stopped by adding 168 μL of Streptavidin-XLent (Cisbio, Cat # 611SAXLA; 1.0 μg mL^{-1}) solution in pH 7.5 dilution buffer made of 0.1 M $NaPO_4$, 0.8 M KF, 1 μg mL^{-1} heparin, and 0.1% BSA. After the mixture was incubated at room temperature for 15 min, 100 μL (per well) of the reaction mixture was transferred to a 384-well microplate (Greiner#781080 384-well) in triplicates and HTRF emissions at 620 nm and 665 nm were measured with 320 nm using Spark 10 M Microplate Reader (Tecan).

Cell viability assay

Human chronic myelogenous leukemia cell line K562 and human cervical cancer cell line HeLa used in our experiments were purchased from Shanghai Cell Bank (Chinese Academy of Science, China). K562 cells were cultured in Iscove's Modified Dulbecco's Medium (IMDM) containing 10% fetal bovine serum (FBS) and 1% penicillin/streptomycin at 37 °C in a humidified incubator containing 5% CO_2. HeLa cells were maintained in modified Eagle's medium (MEM) with 10% FBS and 1% penicillin/streptomycin.

The MTT assay was used in the cell viability. HeLa cells and K562 cells were seeded in 96-well plates at a density of 4000 cells per well, and the cells were incubated with polymer vehicle solution (**GP1–6**) for 72 h at final concentrations of 160 μg mL^{-1}. Then 20 μL of MTT solution (5.0 mg mL^{-1}) was added to the wells and incubated for 4 h at 37 °C. The solution was then discarded, and 150 μL of DMSO were added into the microplate to dissolve the MTT-formazan. The absorbance at 570 nm was measured using a microplate reader (BioTek, Winooski, VT, USA):

$$\text{Cell viability } (\%) = (\text{OD570 test}/\text{OD570 control}) \times 100\%.$$

Confocal microscopy for the localization of GP5-iRGD

HeLa cells were seeded in 24-well plates and treated with 20 μg mL^{-1} of **GP5-iRGD** for 2 h, 4 h, and 12 h, respectively. The cells were then washed twice with PBS and fixed with 4% paraformaldehyde for 1 h. After washing away paraformaldehyde, the cells were stained with 200 μL of DAPI for 10 min. Finally, the DAPI was removed, and the localization of **GP5-iRGD** in the cells was imaged with a confocal microscope.

Fluorescence intensity detection

HeLa cells were incubated with 20 μg mL^{-1} **GP5** and **GP5-iRGD** for different time. The cells were then collected and washed twice with PBS. Fluorescence intensity was detected by flow cytometry (Beckman Coulter, CA, USA).

Western blot analysis

After **GP5-iRGD** treatment, HeLa cells were collected and lysed with loading buffer for 45 min at 4 °C. The lysate was boiled for 15 min and stored at −20 °C. The protein samples were separated by 8% sodium dodecyl sulphate polyacrylamide gels and transferred onto a nitrocellulose filter membrane. The membranes were then incubated with 5% skimmed milk for blocking nonspecific antigenic sites. Afterwards, the membranes were incubated with the corresponding primary antibodies and HRP-conjugated secondary antibodies. Blots were detected using enhanced chemiluminescence solution.

Author contribution

CC, ML and GY conceived the project and designed the experiments; CY, LG and YH synthesized all compounds; MS and YC carried out biological experiments; CY and LG analyzed experimental data and prepared figures with LW, JL and FF; CC and ML wrote the manuscript; RJL and GY revised the manuscript.

Conflicts of interest

There are no conflicts to declare.

Acknowledgements

This research was financially supported by the National Natural Science Foundation of China (81991522 and 21602212), National Key Research and Development Program of China (2017YFE0195000, 2018YFC0310900), National

Science and Technology Major Project for Significant New Drugs Development (2018ZX09735004), NSFC-Shandong Joint Fund for Marine Science Research Centers (U1606403), Shandong Provincial Major Science and Technology Innovation Project (2018SDKJ0404, 2018SDKJ0401), Qingdao National Laboratory for Marine Science and Technology (2016ASKJ08-2), Fundamental Research Funds for the Central Universities (201762002) and Taishan Scholar Project Special Funds.

Notes and references

1 (*a*) R. Sasisekharan and G. Venkataraman, *Biopolymers*, 2000, **4**, 626–631; (*b*) S. Mizuguchi, T. Uyama, H. Kitagawa, K. H. Nomura, K. Dejima, K. Gengyo-Ando, S. Mitani, K. Sugahara and K. Nomura, *Nature*, 2003, **423**, 443–447.

2 (*a*) R. J. Linhardt and T. Toida, *Acc. Chem. Res.*, 2004, **37**, 431–438; (*b*) M. M. Fuster and J. D. Esko, *Nat. Rev. Cancer*, 2005, **5**, 526–542; (*c*) R. Sasisekharan, Z. Shriver, G. Venkataraman and U. Narayanasami, *Nat. Rev. Cancer*, 2002, **2**, 521–528; (*d*) E. J. Bradbury, L. D. F. Moon, R. J. Popat, V. R. King, G. S. Bennett and P. N. Patel, *Nature*, 2002, **416**, 636–640.

3 (*a*) T. H. Nguyen, S.-H. Kim, C. G. Decker, D. Y. Wong, J. A. Loo and H. D. Maynard, *Nat. Chem.*, 2013, **5**, 221–227; (*b*) C. I. Gama, S. E. Tully, N. Sotogaku, P. M. Clark, M. Rawat, N. Vaidehi, W. A. Goddard, A. Nishi and L. C. Hsieh-Wilson, *Nat. Chem. Biol.*, 2006, **2**, 467–473; (*c*) S. Miyata, Y. Komatsu, Y. Yoshimura, C. Taya and H. Kitagawa, *Nat. Neurosci.*, 2012, **15**, 414–422; (*d*) I. Capila and R. J. Linhardt, *Angew. Chem., Int. Ed.*, 2002, **41**, 390–412.

4 R. L. Siegel, K. D. Miller and A. Jemal, *Ca-Cancer J. Clin.*, 2019, **69**, 7–34.

5 (*a*) S. Yamada and K. Sugahara, *Curr. Drug Discovery Technol.*, 2008, **5**, 289–301; (*b*) S. Mizumoto and K. Sugahara, *FEBS J.*, 2013, **280**, 2462–2470.

6 (*a*) G. B. ten Dam, E. M. A. van de Westerlo, A. Purushothaman, R. V. Stan, J. Bulten, F. C. G. J. Sweep, L. F. Massuger, K. Sugahara and T. H. van Kuppevelt, *Am. J. Pathol.*, 2007, **171**, 1324–1333; (*b*) K. N. Sugahara, T. Hirata, T. Tanaka, S. Ogino, M. Takeda, H. Terasawa, I. Shimada, J. Tamura, G. B. ten Dam, T. H. van Kuppevelt, *et al.*, *Cancer Res.*, 2008, **68**, 7191–7199; (*c*) M. J. Vallen, L. F. Massuger, G. B. ten Dam, J. Bulten and T. H. van Kuppevelt, *Gynecol. Oncol.*, 2012, **127**, 202–209.

7 (*a*) C. Mundhenke, K. Meyer, S. Drew and A. Friedl, *Am. J. Pathol.*, 2002, **160**, 185–191; (*b*) R. V. Iozzo and J. D. San Antonio, *J. Clin. Invest.*, 2001, **108**, 349–355; (*c*) C. L. Chu, A. L. Goerges and M. A. Nugent, *Biochemistry*, 2005, **44**, 12203–12213; (*d*) S. S. Deepa, Y. Umehara, S. Higashiyama, N. Itoh and K. Sugahara, *J. Biol. Chem.*, 2002, **277**, 43707–43716.

8 P. Seedevi, M. Moovendhan, S. Vairamani and A. Shanmugam, *Carbohydr. Polym.*, 2017, **167**, 129–135.

9 L. Borsig, L. C. Wang, M. C. M. Cavalcante, L. Cardilo-Reis, P. L. Ferreira, P. A. S. Moura, J. D. Esko and M. S. G. Pavao, *J. Biol. Chem.*, 2007, **282**, 14984–14991.

10 Y. L. Yu, A. Williams, X. Zhang, L. Fu, K. Xia, Y. M. Xu, F. M. Zhang, J. Liu, M. Koffas and R. J. Linhardt, *Glycobiology*, 2019, **29**, 572–581.

11 (*a*) S. B. Peterson and J. Liu, *Matrix Biol.*, 2013, **32**, 223–227; (*b*) I. Vlodavsky and Y. Friedmann, *J. Clin. Invest.*, 2001, **108**, 341–347; (*c*) M. Nakajima, T. Irimura, N. Di Ferrante and G. L. Nicolson, *J. Biol. Chem.*, 1984, **259**, 2283–2290.

12 (*a*) L. Fux, N. Ilan, R. D. Sanderson and I. Vlodavsky, *Trends Biochem. Sci.*, 2009, **34**, 511–519; (*b*) N. Ilan, M. Elkin and I. Vlodavsky, *Int. J. Biochem. Cell Biol.*, 2006, **38**, 2018–2039; (*c*) J. Reiland, D. Kempf, M. Roy, Y. Denkins and D. Marchetti, *Neoplasia*, 2006, **8**, 596–560; (*d*) J. Reiland, R. D. Sanderson and M. Waguespack, *J. Biol. Chem.*, 2004, **279**, 8047–8055.

13 (*a*) E. A. McKenzie, *Br. J. Pharmacol.*, 2007, **151**, 1–14; (*b*) V. Ferro, E. Hammond and J. K. Fairweather, *Mini-Rev. Med. Chem.*, 2004, **4**, 693–702; (*c*) H. Q. Miao, H. Liu, E. Navarro, P. Kussie and Z. Zhu, *Curr. Med. Chem.*, 2006, **13**, 2101–2111.

14 Y. Miura, Y. Hoshino and H. Seto, *Chem. Rev.*, 2016, **116**, 1673–1692.

15 R. Guan, X. L. Sun, S. J. Hou, P. Y. Wu and E. L. Chaikof, *Bioconjugate Chem.*, 2004, **15**, 145–151.

16 (*a*) Y. Miura, K. Yasuda, K. Yamamoto, M. Koike, Y. Nishida and K. Kobayashi, *Biomacromolecules*, 2007, **8**, 2129–2134; (*b*) Y. Nishimura, H. Shudo, H. Seto, Y. Hoshino and Y. Miura, *Bioorg. Med. Chem. Lett.*, 2013, **23**, 6390–6395; (*c*) H. Koide, K. Yoshimatsu, Y. Hoshino, S. Lee, A. Okajima, S. Ariizumi, Y. Narita, Y. Yonamine, A. C. Weisman, Y. Nishimura, N. Oku, Y. Miura and K. J. Shea, *Nat. Chem.*, 2017, **9**, 715–722.

17 J. Li, C. Cai, L. H. Wang, C. D. Yang, H. Jiang, M. M. Li, D. Xu, G. Y. Li, C. X. Li and G. L. Yu, *ACS Macro Lett.*, 2019, **8**, 1570–1574.

18 (*a*) E. T. Sletten, R. S. Loka, F. Yu and H. M. Nguyen, *Biomacromolecules*, 2017, **18**, 3387–3399; (*b*) R. S. Loka, F. Yu, E. T. Sletten and H. M. Nguyen, *Chem. Commun.*, 2017, **53**, 9163–9166; (*c*) R. S. Loka, F. Yu, E. T. Sletten and H. M. Nguyen, *ACS Appl. Mater. Interfaces*, 2019, **11**, 244–254.

19 (*a*) J. H. Ko and H. D. Maynard, *Chem. Soc. Rev.*, 2018, **47**, 8998–9014; (*b*) M. S. Messina, K. M. M. Messina, A. Bhattacharya, H. R. Montgomery and H. D. Maynard, *Prog. Polym. Sci.*, 2020, **100**, 101186.

20 (*a*) Z. Q. Yang, E. B. Puffer, J. K. Pontrello and L. L. Kiessling, *Carbohydr. Res.*, 2002, **337**, 1605–1613; (*b*) L. E. Strong and L. L. Kiessling, *J. Am. Chem. Soc.*, 1999, **121**, 6193–6196.

21 (*a*) R. Okoth and A. Basu, *Beilstein J. Org. Chem.*, 2013, **9**, 608–612; (*b*) S. G. Lee, J. M. Brown, C. J. Rogers, J. B. Matson, C. Krishnamurthy, M. Rawat and L. C. Hsieh-Wilson, *Chem. Sci.*, 2010, **1**, 322–325.

22 (*a*) S. P. Massia and J. A. Hubbell, *J. Cell Biol.*, 1991, **114**, 1089–1100; (*b*) M. Gurrath, G. Muller, H. Kessler, M. Aumailley and R. Timpl, *Eur. J. Biochem.*, 1992, **210**, 911–921.

23 (*a*) A. Zetser, Y. Bashenko, E. Edovitsky, F. Levy-Adam, I. Vlodavsky and N. Ilan, *Cancer Res.*, 2006, **66**, 1455–1463; (*b*) M. D. Hulett, C. Freeman, B. J. Hamdorf, R. T. Baker, M. J. Harris and C. R. Parish, *Nat. Med.*, 1999, **5**, 803–809.